Journal of Advanced Research (2016) 7, 135–141

Cairo University

Journal of Advanced Research

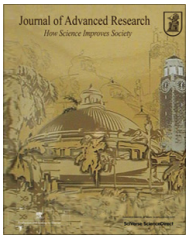

ORIGINAL ARTICLE

Structural, electrical conductivity and dielectric behavior of Na_2SO_4–LDT composite solid electrolyte

Mohd Z. Iqbal, Rafiuddin *

Physical Chemistry Division, Department of Chemistry, Aligarh Muslim University, Aligarh 202002, India

ARTICLE INFO

Article history:
Received 28 November 2014
Received in revised form 30 March 2015
Accepted 3 April 2015
Available online 9 April 2015

Keywords:
Composite solid electrolyte
X-ray diffraction
Differential thermal analysis
Electrical conductivity
Dielectric constant
Dielectric loss

ABSTRACT

A series of composite materials of general molecular formula $(1-x)\ Na_2SO_4-(x)$ LDT was prepared by solid state reaction method. The phase structure and functionalization of these materials were defined by X-ray diffraction (XRD) and Fourier-transform infrared spectroscopy (FT-IR) respectively. Differential thermal analysis (DTA) revealed that the hump of phase transition at 250 °C has decreased while its thermal stability was enhanced. Scanning electron microscopy signifies the presence of improved rigid surfaces and interphases that are accountable for the high ionic conduction due to dispersion of LDT particles in the composite systems. Arrhenius plots of the conductance show the maximum conductivity, $\sigma = 4.56 \times 10^{-4}$ S cm^{-1} at 500 °C for the $x = 0.4$ composition with the lowest activation energy 0.34 eV in the temperature range of 573–773 K. The value of dielectric constant was decreased with increasing frequency and follows the usual trend.

© 2015 Production and hosting by Elsevier B.V. on behalf of Cairo University.

Introduction

Fabrication of composite solid electrolytes having mesoscale interface is an attractive approach for the development of high performance ionic conductors both in fundamental and application point of view [1–3]. The absence of electrolyte leakage, light weight, ease of roll–roll fabrication and improved safety makes the composite solid electrolyte as a suitable candidate for the batteries and electrochemical cells [4]. Dispersion of submicrometer insulating oxide particles such as Al_2O_3, Fe_2O_3, SiO_2, TiO_2 and ZrO_2 is a well known technique to enhance the transport characteristics as well as the thermal and mechanical properties of the several modest ionic conductors at room temperature [5–10]. Generally, ionic conductivity of the solid electrolytes varies with the particle size, concentration and type of the dispersoids. If the particle size of inert component is relatively large then the effect is described satisfactorily by the space charge model [11,12]. If the size of particle of inert component is so small i.e. less than 100 nm then the heterogeneous doping can lead to a significant change in the bulk properties of ionic salts [13]. It has been proposed that the major cause of conductivity enhancement in the composites is due to the strong interaction between matrix and additives. This type of interaction supplies an unusual disordered

* Corresponding author. Tel./fax: +91 571 27034.
E-mail address: rafi_amu@yahoo.co.in (Rafiuddin).
Peer review under responsibility of Cairo University.

http://dx.doi.org/10.1016/j.jare.2015.04.002
2090-1232 © 2015 Production and hosting by Elsevier B.V. on behalf of Cairo University.

state of ionic salts at the interface which depends on the chemical nature and concentration of the composite components. Their morphological characters and energy of interfaces interaction possess unusual bulk properties including high ionic conductivity [14,15]. The ionic conductor/oxide composites may be interpreted by the bulk effects as well as the interfacial influences [16]. Several theoretical models such as space charge layer model, defect-induced order–disorder phase model and random resistor model have been developed by various investigators, satisfactorily explaining the phenomenon of composites in the field of solid state ionics [17,18]. The ionic salt Na_2SO_4 undergoes a phase transition from room temperature phase V to phase I during heating at 250 °C whereas cooling the phase I it transforms to phase III, which subsequently leads to phase V [19]. In this study a series of LDT doped Na_2SO_4 samples i.e. $(1 - x)$ $Na_2SO_4 - (x)$ LDT was prepared by solid state reaction method. Characterizations of these materials were performed by means of the XRD, FTIR, DTA and SEM techniques. The impacts of LDT doping on the electrical and dielectric properties of Na_2SO_4 have been reported.

Experimental

La doped TiO_2 (LDT) in the ratio of 1:5 was synthesized by the procedure which has been reported previously in Ref. [20]. Anhydrous Na_2SO_4 was used from Merck with the purity of 99.99% pure. The required amounts of the raw materials were mixed in an agate mortar and produce the series $(1 - x)$ $Na_2SO_4 - (x)$ LDT, $x = 0$–0.6. The obtained mixtures were then heated in an electrical furnace at 300 °C for 9 h with the intermittent grinding. The final mixtures were crushed to fine powder and hydraulically pelletized by applying the pressure of five tons cm^{-2}.

X-ray diffraction patterns of the prepared samples were recorded by using a Miniflex-II X-ray diffractometer "Rigaku Corporation" with Cu Kα radiations in the 2θ range of 20–80° at room temperature. The unit cell parameters were calculated by using Powder-X program. FTIR analysis of the materials was done by "Interspec 2020 FTIR spectrometer" spectro lab UK, in the wave number range of 4000–400 cm^{-1}.

Differential thermal analysis (DTA) was carried out by "Shimadzu DTG-60H" with heating rate of 20 °C min^{-1} from the temperature 20 to 600 °C in the nitrogen flowing atmosphere. The surface morphology samples were studied by using scanning electron microscopy "Leo 4352" at an accelerating voltage of 20 kV.

The temperature dependent electrical conductivity and dielectric measurements of the samples have been performed by using Wayne Kerr "43100" LCR meter. The heating rate of the sample was controlled by the Eurotherm C-600. To perform the above studies, opposite surfaces of the pelletized samples were sputtered by silver paste to ensure good electrical contact with electrode capacitor. The pellet was annealed between the electrode for 3 h at 420 K before the measurements in order to minimize the grain boundary resistance and to increase the electrical contact between the pellet and electrodes.

Results and discussion

Fig. 1 demonstrates the powder X-ray diffraction patterns of the pure and LDT doped Na_2SO_4 samples at room temperature. It can be clearly seen from the figure that two-phase nature of composite has been obtained. Doping of LDT components has no effects on the peaks position but it only declined the peaks height of the pristine Na_2SO_4. The observed diffraction pattern of the pure Na_2SO_4 sample having an orthorhombic crystal structure with the lattice constant $a = 5.600$ Å, $b = 8.917$ Å, and $c = 6.967$ Å with $\alpha = \beta = \gamma = 90°$. Additionally some new peaks have been detected in case of the composite diffractograms ($x = 0.2$, 0.4 and 0.6), having the lattice constant $a = 3.776$ Å, $c = 9.506$ Å with $\alpha = \beta = \gamma = 90°$, allocate the presence of LDT phase. The composites spectra ($x = 0.2$, 0.4 and 0.6) also show that there is no change takes place in the planes of pristine Na_2SO_4 (except the decrease in heights) with the enhancement of LDT components. The XRD result elucidates that increase in doping concentration developed stresses on the crystal lattice of the composite at microscopic level which results the decrease in crystallinity and peak intensity of samples that enhance the disorder effect. The refined unit cell parameters and unit cell volumes for the pure and doped samples are presented in Table 1. Here we observed from the table that reduction in these values occurs due to the increase of LDT contents. This is because of the decrease in crystallite size as well as peak intensity of the samples with the addition of LDT particles.

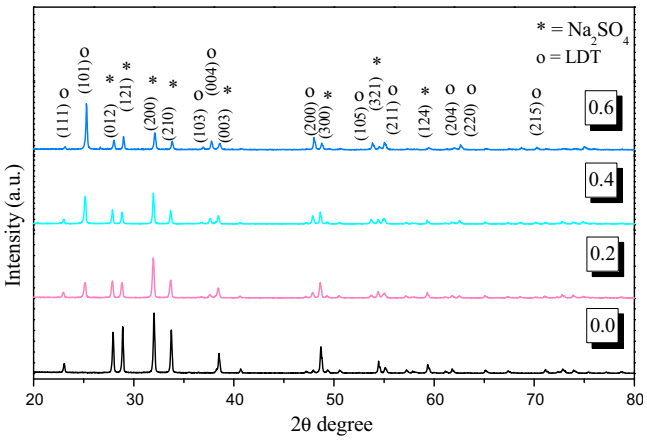

Fig. 1 Room temperature X-ray diffractograms of $(1 - x)$ $Na_2SO_4 - (x)$ LDT samples.

FT-IR spectra of the composite samples at room temperature are presented in Fig. 2. The pure Na_2SO_4 sample shows the strong IR absorption band observed at the wave number 3450.60 cm^{-1} is due to the OH stretching of HSO_4 group while a band around 2150.00 cm^{-1} assigns the υ_3 of H_2O molecule. It

Table 1 Calculated lattice parameters and unit cell volumes of the orthorhombic Na_2SO_4 at room temperature in the $(1 - x)$ $Na_2SO_4 - (x)$ LDT composite system.

Sample	Lattice parameter (Å)			Unit cell volume (Å)
	a	*b*	*c*	
$X = 0.0$	5.600	8.917	6.967	347.90
$X = 0.2$	5.590	8.934	6.966	347.89
$X = 0.4$	5.579	8.946	6.966	347.67
$X = 0.6$	5.578	8.945	6.965	347.52

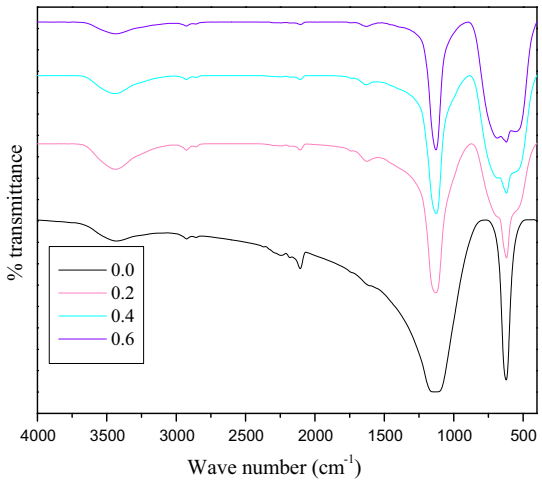

Fig. 2 Room temperature FT-IR spectra of $(1-x)$ $Na_2SO_4 - (x)$ LDT samples.

can be also seen from the spectra that IR band at 1134.00 cm^{-1} explains the asymmetric stretching whereas the band at 621.94 cm^{-1} allocates the asymmetric bending of the SO_4 group. In the case of composites some new IR bands are also observed at 682.68 cm^{-1} and 528.67 cm^{-1} attributed to the LDT particles [21]. The IR result summarized that the vibrational bands of water molecules present in all spectra arises from the atmospheric moisture during the KBr pellet formation. The KBr component is highly hygroscopic in nature and it can easily absorb moisture from the surrounding. It can be also seen from the spectra that increase of LDT contents, results the decrease of the sharpness of absorption band of composite samples. It is well known that decrease of sharpness of absorption bands revealed the presence of crystallographic disordering responsible for the variation in bulk properties of such composites.

Fig. 3 displays the DTA curves of the pure and LDT doped Na_2SO_4 samples with the heating rate of 20 °C/min. The thermogram of the pure Na_2SO_4 shows that the endothermic peak at the temperature 250 °C corresponds to the phase transition from phase V → I [19]. It is interesting to note that, introduction of LDT components into the crystal lattice of Na_2SO_4

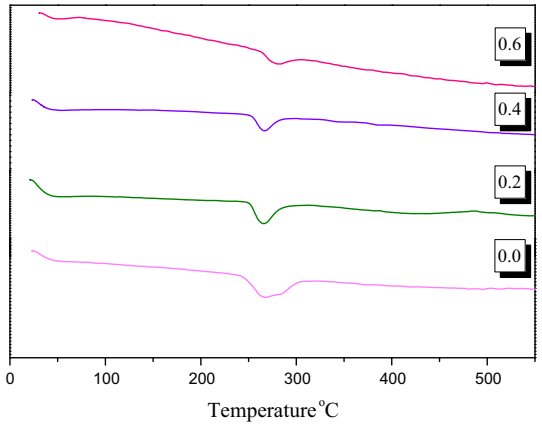

Fig. 3 DTA thermograms of the $(1-x)$ $Na_2SO_4 - (x)$ LDT samples.

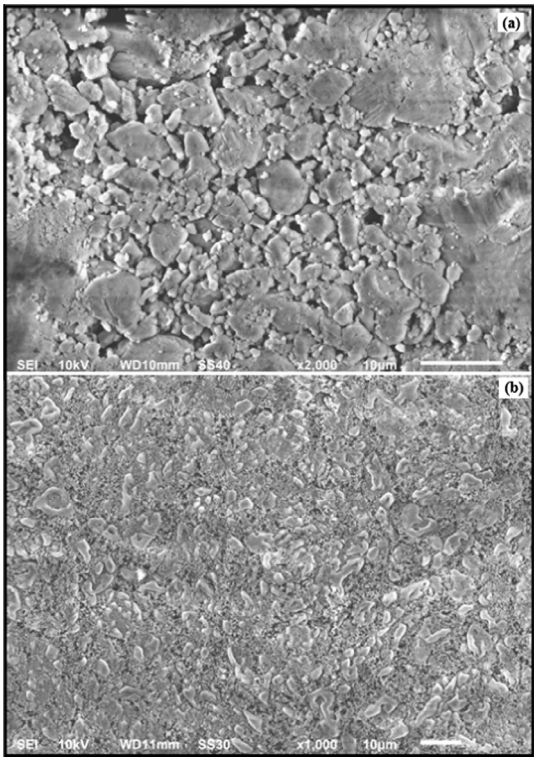

Fig. 4 SEM micrograph (a) $x = 0.0$ & (b) $x = 0.3$ mol fraction of the $(1-x)$ $Na_2SO_4 - (x)$ LDT composite solid electrolytes.

induces small changes i.e. the endothermic peak of solid electrolyte has been disappeared sufficiently at higher concentration of LDT additives. This may be caused by the transformation of a crystalline phase to an interface-stabilized amorphous state which is responsible for the high ionic conduction in composite. This type of behavior was also reported previously by others in several composite systems such as $TlI–TiO_2$ and $Cs_3(H_2PO_4)(HSO_4)_2–SiO_2$ [22,23].

Scanning electron micrograph for the pure Na_2SO_4 is shown in Fig. 4(a). After the preparation of composite, SEM micrograph of composite ($x = 0.3$) sample is presented in Fig. 4(b) to understand the distribution of LDT particles in the salt matrix. It can be seen from the micrograph that submicrometric LDT particles were distributed throughout the sulfate phase. It simply improves the grain–grain contacts and provides better mechanical properties. The SEM image of the composite sample reveals the presence of rigid surfaces in the system due to the dispersion of LDT particles. The existence of these additional surfaces and interphases enhanced the ionic conduction in composite. Such type of interactions between the ionic salts and metal oxides called as space charge layer that transform the bulk properties of solid electrolyte [24].

Fig. 5 exhibits electrical conductivity behavior for $(1-x)$ $Na_2SO_4 - (x)$ LDT composite solid electrolytes at different temperatures and compositions. The conductivity was increased due to the enrichment of LDT content reaching a highest value with 40%, thereafter it decreases with further increase in amount of LDT content. High value of conductivity may be attributed either due to the formation of a highly conducting phase along the interface or the formation of a highly conducting space-charge layer along the normal

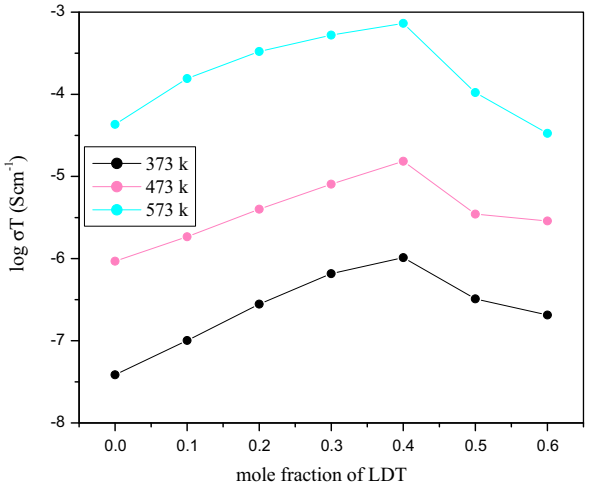

Fig. 5 Electrical conductivity as a function of composition of $(1-x)\ Na_2SO_4-(x)$ LDT samples at different temperatures.

conductor–insulator interface. At very high volume fractions of dispersing oxide, this type of distribution must change and acts blocking for the interfacial transport.

The temperature dependence of ionic conductivity is given by the Arrhenius expression as

$$\sigma_T = \sigma_0 \times \mathrm{Exp}\left(\frac{-Ea}{KT}\right) \tag{1}$$

where σ_0 is pre-exponential factor and Ea is the activation energy of ionic motion. As shown in Fig. 6 an abrupt change in conductivity has been found in case of pristine Na_2SO_4 at 523 K during heating due to the phase transition from phase V to phase I. Addition of fine LDT particles leads to increase in the conductivity at given temperature with x up to 0.4, and thereafter reduction in conductivity occurs as we further increase the mole fraction of LDT content. The abrupt change due to order–disorder phase transition in the conductivity disappeared at higher concentration of this oxide additive and the curves tend to be straight along the whole temperature region in this study. The activation energies of conduction at high

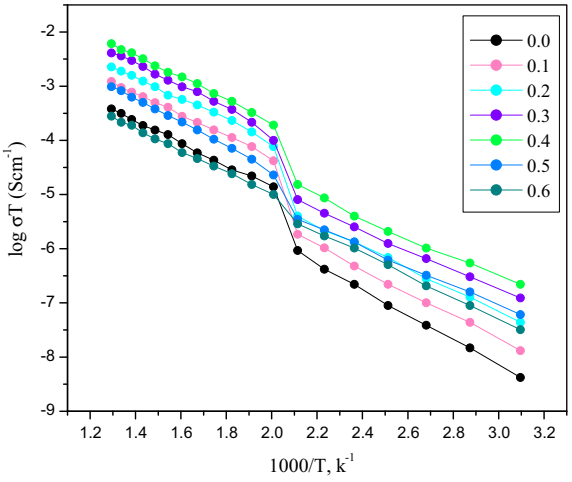

Fig. 6 Electrical conductivity as a function of temperature of $(1-x)\ Na_2SO_4-(x)$ LDT samples.

Table 2 Activation energies of conduction in the temperature range 573–773 K of $(1-x)\ Na_2SO_4-(x)$ LDT composite system.

Sample	Activation energy (eV)
$X = 0.0$	0.50
$X = 0.1$	0.43
$X = 0.2$	0.44
$X = 0.3$	0.36
$X = 0.4$	0.34
$X = 0.5$	0.45
$X = 0.6$	0.52

temperature regions were obtained by linear square fitting to Arrhenius plot in the temperature range 573–773 K are listed in Table 2. It can be concluded from the table that activation energies were found to be composition dependent. The values of this energy were decreased with increase of dopant concentrations and follow the opposite trend of the conductivity.

Dielectric properties of solid materials can be well explained as a function of frequency of applied electric field, temperature, crystal structure and other parameters. The dielectric constant of a material is represented by

$$\varepsilon = \varepsilon' - j\varepsilon'' \tag{2}$$

where ε' and ε'' are the real and imaginary part of dielectric constant, representing the amount of energy stored in a dielectric material as polarization and energy loss respectively [25,26]. The frequency dependent real part of dielectric constant (ε') can be calculated by using the relation

$$\varepsilon' = \frac{Cpt}{\varepsilon_0 A} \tag{3}$$

where Cp is the capacitance of the specimen in Farad (F), t is thickness of pellet, ε_0 is the permittivity of free space (8.854×10^{-12} F/m) and A is the area of the flat surface of the pellet.

The complex or imaginary part of the dielectric constant (ε'') can be obtained by the equation

$$\varepsilon'' = \varepsilon' \tan\delta \tag{4}$$

where $\tan\delta$ is called as the dielectric loss tangent which is proportional to the loss of energy dissipated as heat from the applied field into the sample. Dielectric constant (real and imaginary) and dielectric loss for the selected samples over various frequencies at the temperature 200 °C are depicted in Fig. 7(a)–(c). It is observed from the figure that both real and imaginary parts of dielectric constants as well as dielectric loss of the samples have been decreased exponentially with frequency and showed the frequency independent behavior at higher frequency. These properties were improved with rise in mole fraction of LDT and attain a maximum value at $x = 0.4$, later it starts to decrease with further increase of LDT contents. The increase in the value of dielectric constants is due to the increase in the ion conduction related polarization [27]. The heterogeneous dispersion of LDT particles leads to a significant increase of conductivity in the low temperature region. The composition $x = 0.6$ has the more conductivity compared to the pure salt at low temperature region and has the more dielectric value. The dielectric loss is found to

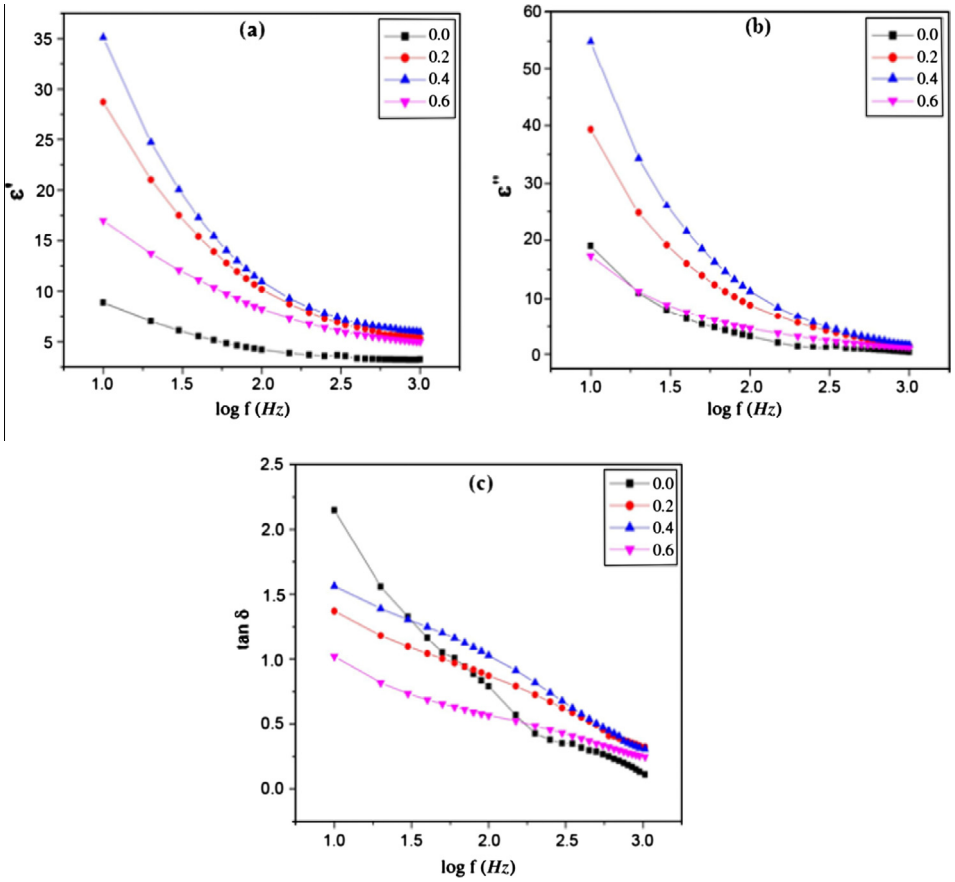

Fig. 7 Variation of (a) real part of dielectric constant, (b) imaginary part of dielectric constant and (c) dielectric loss at 200 °C for different concentrations.

decrease much faster than dielectric constant in the low frequency region and the variation is same as in higher frequency region. The enhancement in dielectric loss by increasing x ascribed the improvement in motion of Na^+ ions.

The phenomenon of dielectric dispersion has been well explained on the basis of Maxwell–Wagner model [28,29] and Koop's phenomenological theory [30]. In this model, a dielectric medium has been assumed which is made up of well conducting grains and poorly conducting grain boundaries respectively. The grains are highly conductive and have high values of permittivity, while the grain boundaries are less conductive and have smaller values of permittivity. At low frequency region grain boundaries are more effective than the grains in electrical conduction. Thinner the grain boundary results the higher value of dielectric constant. Higher values of the dielectric constant observed at lower frequencies have been also explained on the basis of interfacial/space polarization due to nonhomogeneous dielectric structure [31].

High values of ε' at low frequency region irrespective of temperature of measurements can be attributed due to the accumulation of charge at the electrode and electrolyte interface, because ions are unable to exchange with silver electrodes [32]. As the frequency increases, ε' decreases because of high periodic reversal of the field at the interface which reduces the contribution of charge carriers toward the dielectric constant and finally, ε' saturates at high frequency giving rise to dielectric constant of the material [33]. Moreover the experimental results were well explained the behavior of the dielectric properties as a function of frequency for the intermediate composition $x = 0.3$ at different temperatures in Fig. 8(a)–(c). The composite material shows the enhancement in the values of dielectric constant and dielectric loss with temperature. The maximum value of dielectric constant was obtained at the temperature 573 K under the investigated temperature. The behavior of ε' in the present investigations is typical of polar dielectric, where jump orientation effect and space charge polarization were facilitated by the increased temperature resulting in increased dielectric properties and conductivity of the composites [34,35]. The dielectric constant of the composite samples as function of temperature at 300 kHz is shown in Fig. 9. The dielectric constant of the composite electrolytes increases apparently with the increase of temperature in the entire temperature range under this study. The plot shows that a sharp increase of dielectric constant takes place at 523 K over the investigated temperature. The abrupt change in dielectric constant has been verified by the conductivity and DTA measurements around the same temperature. The low value of the dielectric constant at low temperature ascribed to the electronic contribution and the absence of significant number of space-charge polarization and ionic jump orientation, which create the pathway suitable for migration of Na^+ ions. The huge increase in the value of dielectric constant irrespective of temperature can be attributed to the number of charge carriers sharply enhanced above 523 K, and orientation of dipole has facilitated leading to increase in ionic-jump orientation and space-charge polarization [36].

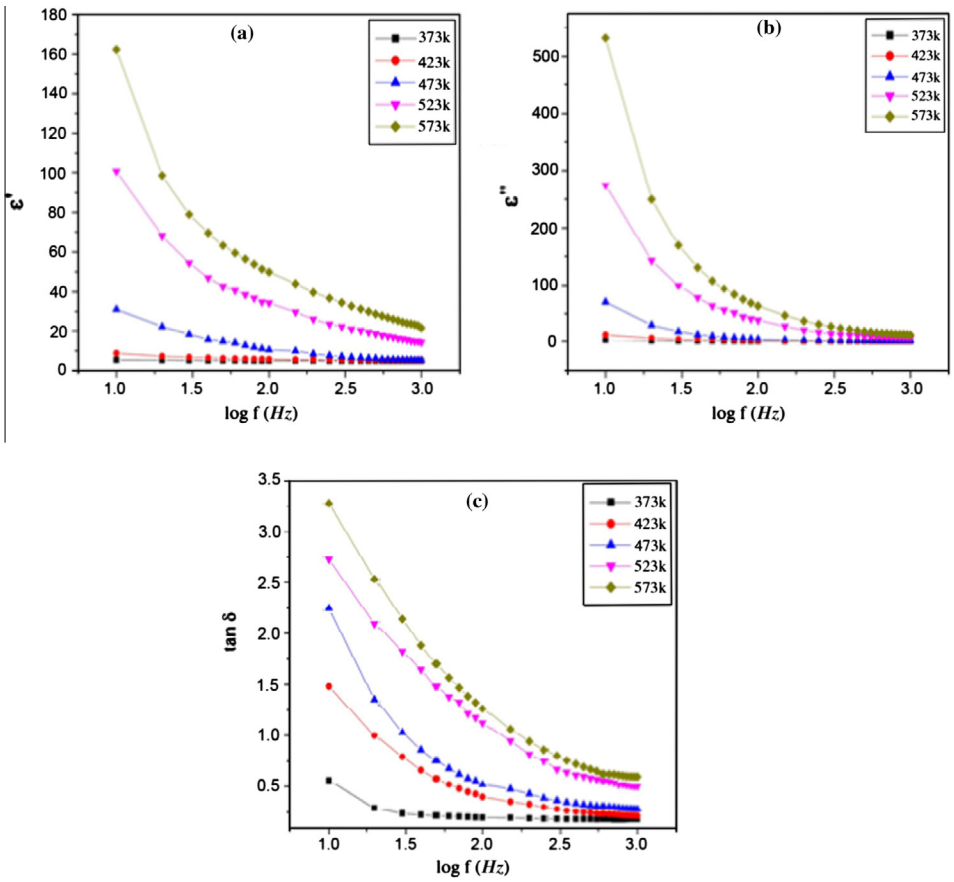

Fig. 8 Variation of (a) real part of dielectric constant, (b) imaginary part of dielectric constant and (c) dielectric loss for $x = 0.3$ mol fraction at different temperatures.

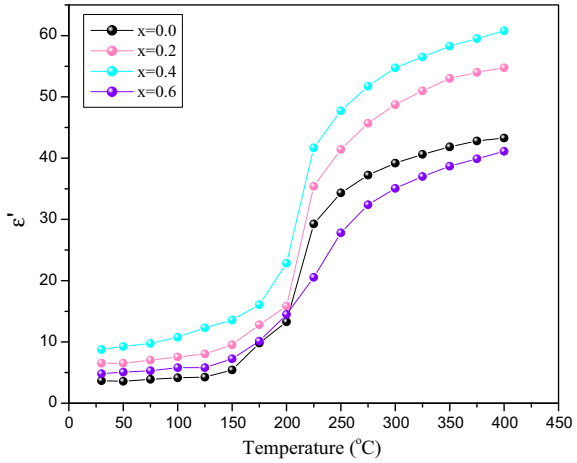

Fig. 9 Temperature dependence of dielectric constant of $(1 - x)$ $Na_2SO_4 - (x)$ LDT samples.

Conclusions

Two phase nature of the composite material was confirmed by XRD and FT-IR analysis significantly. Thermal analysis explains that the hump of phase transition was effectively decreased which may be caused by the transformation of crystalline phase to an interface-stabilized amorphous phase. The SEM analysis screening improved surfaces and interphases responsible for the high ionic conduction. The conductivity of the composite was enhanced while activation energy was decreased as compared to the pure Na_2SO_4. Maximum value of conductivity and dielectric constants was observed for the $x = 0.4$ composite sample under this study. The dielectric constants and dielectric loss were enhanced with the increase of LDT component as well as the temperature, while it decreases irrespective of increasing frequency. The huge increase in the value of dielectric constant irrespective of temperature has been satisfactorily explained on the basis of ionic-jump orientation and space-charge polarization.

Conflict of interest

The authors have declared no conflict of interest.

Compliance with Ethics Requirements

This article does not contain any studies with human or animal subjects.

Acknowledgments

The authors are gratefully acknowledged the chairman, Department of Chemistry for providing research facilities and UGC, New Delhi for financial support. We are also thanking to Department of Physics AMU, Aligarh for XRD analysis.

References

[1] Maekawa H, Iwatani T, Shen H, Yamamura T, Kawamura J. Enhanced lithium ion conduction and the size effect on interfacial phase in Li_2ZnI_4–mesoporous alumina composite electrolyte. Solid State Ionics 2008;178:1637–41.

[2] Maier J. Ionic conduction in space charge region. Prog Solid State Chem 1995;23:171–263.

[3] Tuller HL. Ionic conduction in nanocrystalline materials. Solid State Ionics 2000;131:143–57.

[4] Vignarooban K, Dissanayake MAKL, Albinsson I, Mellander BE. Effect of TiO_2 nano-filler and EC plasticizer on electrical and thermal properties of poly (ethylene oxide) (PEO) based solid polymer electrolytes. Solid State Ionics 2014;266:25–8.

[5] El-Shaarawy MG. Physical studies on composites $Ag_7I_4VO_4$–Al_2O_3. J Phys Chem Solids 2005;66:1247–51.

[6] Uvarov NF, Shrivastava OP, Hairetdinov EF. Composite solid electrolytes in the Li_2SO_4–Al_2O_3 system. Solid State Ionics 1989;36:39–42.

[7] Rogeza J, Schaf O, Knauth P. What can calorimetry contribute to the understanding of vitreous and composite solid electrolytes. Solid State Ionics 2000;136:955–9.

[8] Diosa JE, Solis A, Vargas RA, Mellander BE. Effect of dispersed Al_2O_3 on the phase transitions and ionic conductivity of $KHSO_4$. Solid State Ionics 2004;175:459–61.

[9] Huang MR, Ding YB, Li XG, Liu YJ, Xi K, Gao CL, Kumar RV. Synthesis of semiconducting polymer microparticles as solid ionophore with abundant complexing sites for long-life Pb (II) sensors. ACS Appl Mater Interfaces 2014;6:22096–107.

[10] Huang MR, Ding YB, Li XG. Lead-ion potentiometric sensor based on electrically conducting microparticles of sulfonic phenylenediamine copolymer. Analyst 2013;138:3820–9.

[11] Maier J. Space charge regions in solid two-phase systems and their conduction contribution-I. Conductance enhancement in the system ionic conductor-'inert' phase and application on AgCl:$A1_2O_3$, and AgCl:SiO_2. J Phys Chem Solids 1985;46:309–20.

[12] Wagner Jr JB. High conductivity solid ionic conductors. Singapore: World Scientific; 1989, p. 146.

[13] Uvarov NF, Vangk P, Yuzyuk YI, Zelezny V, Studnicka V, Bokhonov, et al. Properties of rubidium nitrate in ion-conducting $RbNO_3$–Al_2O_3 nanocomposites. Solid State Ionics 1996;90:201–7.

[14] Ponomareva VG, Lavrova GV. The investigation of disordered phases in nanocomposite proton electrolytes based on $MeHSO_4$ (Me = Rb, Cs, K). Solid State Ionics 2001;145:197–204.

[15] Lavrova GV, Ponomareva VG, Uvarov NF. Nanocomposite ionic conductors in the system $MeNO_3$–SiO_2 (Me = Rb, Cs). Solid State Ionics 2000;136:1285–9.

[16] Uvarov NF, Maier J. EMF Study of thermodynamic properties of AgC1–$A1_2O_3$ composite solid electrolytes and low temperature conductivity. Solid State Ionics 1993;62:251–6.

[17] Uvarov NF, Isupov VP. Effect of morphology and particle size on the ionic conductivities of composite solid electrolytes. Solid State Ionics 1992;51:41–52.

[18] Rao MVM, Reddy SN, Chary AS. DC ionic conductivity of $NaNO_3$: γ-Al_2O_3 composite solid electrolyte system. Physica B 2005;362:193–8.

[19] Bobade SM, Kulkarni AR, Gopalan P. Electrical properties of Na_2SO_4-based composite systems. Ionics 2007;13:257–62.

[20] Umar K, Haque MM, Muneer M, Harada T, Matsumura M. Mo, Mn and La doped TiO_2: synthesis, characterization and photocatalytic activity for the decolourization of three different chromophoric dyes. J Alloys Compd 2013;578:431–8.

[21] Mohamed MM, Bayoumy WA, Khairy M, Mousa MA. Synthesis and structural characterization of TiO_2 and V_2O_5/TiO_2 nanoparticles assembled by the anionic surfactant sodium dodecyl sulphate. Microporous Mesoporous Mater 2006;97:66–77.

[22] Sultana S, Rafiuddin. Electrical conductivity in TlI–TiO_2 composite solid electrolyte. Physica B 2009;404:36–40.

[23] Ponomareva VG, Shutova ES. Composite electrolytes $Cs_3(H_2PO_4)$ $(HSO_4)_2/SiO_2$ with high proton conductivity. Solid State Ionics 2005;176:2905–8.

[24] Sultana S, Rafiuddin. Electrical properties of V_2O_5-doped TlI. Radiat Effect Defects Solids 2009;164:771–8.

[25] Hassan MM, Ahmed AS, Chaman M, Khan W, Naqvi AH, Azam A. Structural and frequency dependent dielectric properties of Fe^{3+} doped ZnO nanoparticles. Mater Res Bull 2012;47:3952–8.

[26] Ansari SA, Nisar A, Fatma B, Khan W, Naqvi AH. Investigation on structural, optical and dielectric properties of Co doped ZnO nanoparticles synthesized by gel-combustion route. Mater Sci Eng B 2012;177:428–35.

[27] Ahamad MN, Varma KBR. Dielectric properties of $(100 - x)$ $Li_2B_4O_7$ $x(Ba_5Li_2Ti_2Nb_8O_{30})$ glasses and glass nanocrystal composites. Mater Sci Eng B 2010;167:193–201.

[28] Maxwell JC. Electricity and magnetism. Oxford University Press 1873;1:328.

[29] Wagner K. Theorie der unvolkommenen dielektrika. Ann Phys 1913;40:817–55.

[30] Koop's C. On the dispersion of resistivity and dielectric constant of some semiconductors at audio frequencies. Phys Rev 1951;83:121–4.

[31] Batoo KM, Kumar S, Lee CG, Alimuddin. Influence of Al doping on electrical properties of Ni–Cd nano ferrites. Curr Appl Phys 2009;9:826–32.

[32] Hodge LM, Ingram MD, West AR. Impedance and modulus spectroscopy of polycrystalline solid electrolytes. J Electroanal Chem 1976;74:125–43.

[33] Anantha PS, Hariharan K. Ac conductivity analysis and dielectric relaxation behaviour of $NaNO_3$–Al_2O_3 composite. Mater Sci Eng B 2005;121:12–9.

[34] Nawaz MS, Rafiuddin. Ionic conduction and effect of cation doping in Tl_4HgI_6. Ionics 2007;13:35–40.

[35] Ravi M, Pavani Y, Kumar KK, Bhavani S, Sharma AK, Rao VVRN. Studies on electrical and dielectric properties of PVP:KBr O4 complexed polymer electrolyte film. Mater Chem Phys 2011;130:442–8.

[36] Tareev B. Physics of dielectric materials. Moscow: Mir; 1979.